ELSEVIER

Signal Processing 51 (1996) 93–104

SIGNAL PROCESSING

A novel approach to detection of closely spaced sinusoids

Hsiang-Tsun Li, Petar M. Djurić*

Department of Electrical Engineering, State University of New York at Stony Brook, Stony Brook, NY 11794-2350, USA

Received 17 February 1995; revised 25 August 1995 and 6 February 1996

Abstract

A novel method for the detection of closely spaced sinusoids is proposed. It is based on the notch periodogram and a simple detection criterion. Compared with other well-known approaches, this method is not as sensitive to the accuracy of the estimated signal parameters, and it can be implemented with a low computational load. Simulation results of the approach are included, and they show excellent performance.

Zusammenfassung

Eine neue Methode zur Detektion dicht benachbarter Sinussignale wird vorgeschlagen. Sie basiert auf dem Notch-Periodogramm und einem einfachen Detektions-Kriterium. Verglichen mit anderen bekannten Ansätzen ist diese Methode unempfindlich bezüglich der Genauigkeit der geschätzten Signal-parameter und sie kann mit nur geringer Rechenleistung implementiert werden. Simulationsergebnisse zu dem gewählten Ansatz werden vorgestellt; sie zeigen ein hervorragendes Verhalten.

Résumé

Une méthode innovatrice est proposée pour la détection de sinusoïdes rapprochées. Elle est basée sur le périodogramme à bande étroite coupée et un critère de détection simple. Comparée avec d'autres approches bien connues, cette méthode n'est pas aussi sensible à la précision des paramètres estimés du signal, et elle peut être implantée avec une charge de calcul minimale. Des résultats de simulation de l'approche sont inclus, et ils montrent d'excellentes performances.

Keywords: Detection; Notch periodogram; Frequency estimation; Projection matrices; Hypothesis testing; FFT

1. Introduction

Signal detection is an important research area in signal processing with a broad range of applications. Of special interest in many signal processing problems is the detection of sinusoids in noise. The detection of well-resolved sinusoids has been presented for example in [12]. A more difficult problem, however, is the detection of sinusoids with close frequencies. Currently, a popular approach for resolving this problem is to employ an information theoretic criterion, such as the Akaike's Information Criterion (AIC) [2, 14] or the

* Corresponding author. Tel.: 516 632 8423; fax: 516 632 8494; e-mail: djuric@sbee.sunysb.edu.

PII S0165-1684(96)00034-5

Minimum Description Length (MDL) rule [13, 16]. However, the results obtained by these methods are not satisfactory, and the computational cost for implementing them is considerably high. Other methods are based on Bayesian theory [4, 8], and they show excellent performance, but unfortunately are also computationally intensive.

It is well known that specific sinusoidal components can be removed by employing ideal band-stop filters. If the band-stop frequency of one such filter is set at the peak of the data's periodogram, the spectrum of its output around the notch frequency is either flat or with peaks. It is flat if the periodogram peak corresponds to one sinusoidal component, and with peaks if the periodogram peak contains multiple sinusoids. This observation has motivated the present work and had led to the use of the notch periodogram. In this paper, based on the *notch periodogram*, we propose an efficient and simple approach for *detection* (NPD) of the number of sinusoids in each periodogram peak. Compared with other well-known methods, this approach does not require very precise estimation of the signal parameters. Its important feature is that it can be implemented by an FFT procedure [6, 7], and therefore is computationally very efficient. Our analysis of the algorithm also provides the effects of the phases and amplitudes on the resolution of two sinusoids. Despite the periodogram's limited resolution, we show that the method can achieve marked results in detecting sinusoids including the cases of closely spaced sinusoids with different amplitudes. Simulation results are presented, and they demonstrate excellent performance of the proposed algorithm.

The paper is organized as follows. In Section 2 we formulate the problem, and in Section 3 we present some relevant results for our main analysis. The derivation of the algorithm is given in Section 4 and its summary in Section 5. This is followed by simulation results in Section 6 and brief concluding remarks in Section 7.

2. Problem statement

A vector of measurements, $\boldsymbol{y}$, is observed whose components are samples of m complex sinusoids corrupted by additive white Gaussian noise, i.e.,

$$y[n] = \sum_{i=1}^{m} a_i \exp(\mathrm{j}2\pi f_i n) + \varepsilon[n], \tag{1}$$

where $n = 0, 1, 2, \ldots, N-1$; $a_i, f_i, i = 1, 2, \ldots, m$, are the complex amplitude and frequency of the ith sinusoid and $\mathrm{j} = \sqrt{-1}$. The random samples $\varepsilon[n]$ are complex independent, and identically distributed. Moreover, the real and imaginary components of $\varepsilon[n]$ are identically normally distributed with zero mean and unknown variance $\sigma^2/2$. The number m of sinusoids is also unknown. It is assumed that the sinusoids are clustered in l groups, and within each group they cannot be resolved by the periodogram whose resolution limit for complex data is $(2N)^{-1}$. If each group contains m_k sinusoids, $k = 1, 2, \ldots, l$, we rewrite (1) as

$$y[n] = \sum_{k=1}^{l} \sum_{i=1}^{m_k} a_i^{(k)} \exp(\mathrm{j}2\pi f_i^{(k)} n) + \varepsilon[n], \tag{2}$$

where $a_i^{(k)}$ and $f_i^{(k)}$ are the parameters of the ith sinusoid from the kth group, and $\sum_{k=1}^{l} m_k = m$. In other words, the periodogram of (1) has l distinct peaks, i.e., l groups of sinusoids. The problem is to determine the number m_k of sinusoids in each peak of the periodogram.[1]

3. Preliminaries

The observed samples can be represented in a vector–matrix form by

$$\boldsymbol{y} = \sum_{i=1}^{m} a_i \boldsymbol{d}(f_i) + \boldsymbol{\varepsilon} = \sum_{i=1}^{m} \boldsymbol{s}_i + \boldsymbol{\varepsilon}, \tag{3}$$

where

$$\boldsymbol{d}(f_i)^{\mathrm{T}} = [1 \;\; \exp(\mathrm{j}2\pi f_i) \;\; \exp(\mathrm{j}4\pi f_i) \;\; \ldots \exp(\mathrm{j}(N-1)2\pi f_i)],$$

with the superscript T denoting transposition, and $\boldsymbol{s}_i = a_i \boldsymbol{d}(f_i), i = 1, 2, \ldots, m$. In the remaining part of the paper, for notational convenience, whenever

[1] Note that we assume the peaks have already been detected, for example, by the approach in [12].

there is no ambiguity, $\boldsymbol{d}(f)$ will be denoted as $\boldsymbol{d}$. Let the projection operator $\boldsymbol{P}$ spanning the space of $\boldsymbol{d}$ be denoted as $\boldsymbol{P}_{\{\boldsymbol{d}\}}$ or $\boldsymbol{P}(f)$, where $\boldsymbol{P}(f) = \boldsymbol{d}(\boldsymbol{d}^{\mathrm{H}}\boldsymbol{d})^{-1}\boldsymbol{d}^{\mathrm{H}}$, with the superscript H denoting conjugate transposition. Then the orthogonal projection operator $\boldsymbol{P}^{\perp}(f)$ is defined as $\boldsymbol{P}^{\perp}(f) = \boldsymbol{I} - \boldsymbol{P}(f)$. In the sequel we will use the following result of orthogonal subspace decomposition [5]:

$$\{\boldsymbol{x}_1\} \oplus \{\boldsymbol{x}_2\} = \{\boldsymbol{x}_1\} \oplus \{\boldsymbol{P}_{\boldsymbol{x}_1}^{\perp}\boldsymbol{x}_2\}, \tag{4}$$

where $\boldsymbol{x}_1, \boldsymbol{x}_2 \in \mathbb{R}^N$, and $\{\boldsymbol{x}_1\} \oplus \{\boldsymbol{x}_2\}$ denotes the space spanned by $\boldsymbol{x}_1$ and $\boldsymbol{x}_2$. The space spanned by $\boldsymbol{x}_1$ and $\boldsymbol{x}_2$ can be decomposed into the orthogonal spaces spanned by $\boldsymbol{x}_1$ and $\boldsymbol{P}_{\boldsymbol{x}_1}^{\perp}\boldsymbol{x}_2$, or

$$\boldsymbol{P}_{\{\boldsymbol{x}_1\} \oplus \{\boldsymbol{x}_2\}} = \boldsymbol{P}_{\{\boldsymbol{x}_1\}} + \boldsymbol{P}_{\{\boldsymbol{P}_{\boldsymbol{x}_1}^{\perp}\boldsymbol{x}_2\}}, \tag{5}$$

where

$$\boldsymbol{P}_{\boldsymbol{x}_1}\boldsymbol{P}_{\{\boldsymbol{P}_{\boldsymbol{x}_1}^{\perp}\boldsymbol{x}_2\}} = \boldsymbol{0}.$$

Now, we can use (5) to express the projection matrix $\boldsymbol{P}(f, f_n)$ which spans the space of $\boldsymbol{d}(f)$ and $\boldsymbol{d}(f_n)$ as

$$\begin{aligned} \boldsymbol{P}(f, f_n) &= \boldsymbol{P}(f_n) + \boldsymbol{P}^{\perp}(f_n)\boldsymbol{d}(f) \\ &\quad \times (\boldsymbol{d}^{\mathrm{H}}(f)\boldsymbol{P}^{\perp}(f_n)\boldsymbol{d}(f))^{-1}\boldsymbol{d}^{\mathrm{H}}(f)\boldsymbol{P}^{\perp}(f_n). \end{aligned} \tag{6}$$

Next, using vector–matrix notation we define the notch periodogram [6] and the periodogram [10] of $\boldsymbol{y}$ respectively as

$$\begin{aligned} P_n(f; f_n) &= \boldsymbol{y}^{\mathrm{H}}(\boldsymbol{P}(f, f_n) - \boldsymbol{P}(f_n))\boldsymbol{y} \\ &= \boldsymbol{y}^{\mathrm{H}}\boldsymbol{P}^{\perp}(f_n)\boldsymbol{d}(\boldsymbol{d}^{\mathrm{H}}\boldsymbol{P}^{\perp}(f_n)\boldsymbol{d})^{-1}\boldsymbol{d}^{\mathrm{H}}\boldsymbol{P}^{\perp}(f_n)\boldsymbol{y} \\ &= \boldsymbol{y}^{\mathrm{H}}\tilde{\boldsymbol{d}}(f, f_n)(\tilde{\boldsymbol{d}}^{\mathrm{H}}(f, f_n)\tilde{\boldsymbol{d}}(f, f_n))^{-1}\tilde{\boldsymbol{d}}^{\mathrm{H}}(f, f_n)\boldsymbol{y} \\ &= \boldsymbol{y}^{\mathrm{H}}\boldsymbol{P}_{\tilde{\boldsymbol{d}}}(f, f_n)\boldsymbol{y}, \end{aligned} \tag{7}$$

where f_n is the notch frequency and $\tilde{\boldsymbol{d}}(f, f_n) = \boldsymbol{P}^{\perp}(f_n)\boldsymbol{d}$, and

$$P_{\mathrm{per}}(f) = \boldsymbol{y}^{\mathrm{H}}\boldsymbol{P}(f)\boldsymbol{y}. \tag{8}$$

Let now $\Delta = f - f_n$. Then it is not difficult to show that

$$\boldsymbol{d}^{\mathrm{H}}\boldsymbol{P}^{\perp}(f_n)\boldsymbol{d} = \tilde{\boldsymbol{d}}^{\mathrm{H}}\tilde{\boldsymbol{d}} = N'(\Delta), \tag{9}$$

where

$$N'(\Delta) = N - \frac{1}{N}\frac{1 - \cos(2\pi\Delta N)}{1 - \cos(2\pi\Delta)} \tag{10}$$

and that the notch periodogram can be expressed as

$$P_n(f, f_n) = \begin{cases} \dfrac{1}{N'(\Delta)}|\boldsymbol{d}^{\mathrm{H}}\boldsymbol{P}^{\perp}(f_n)\boldsymbol{y}|^2, & \Delta \neq 0, \\ 0, & \Delta = 0. \end{cases} \tag{11}$$

It is important to note that when $\boldsymbol{d}(f)$ and $\boldsymbol{d}(f_n)$ are orthogonal, $P_n(f; f_n) = P_{\mathrm{per}}(f)$. Also, if $\boldsymbol{y} = \boldsymbol{\varepsilon}$ and $f \neq f_n$, one can readily deduce from (7) that $2P_n(f; f_n)/\sigma^2$ has the central chi-squared probability density function (p.d.f.) with two degrees of freedom, that is,

$$\frac{2P_n(f; f_n)}{\sigma^2} \sim \chi_2^2. \tag{12}$$

(For more details, cf. Appendix A.)

We can also define a notch periodogram with more than one notch. In the case of q notch components, we replace the notch frequency f_n by a notch vector $\boldsymbol{f}_n = [f_{n1}\ f_{n2}\ \dots f_{nq}]$ and write

$$\begin{aligned} P_n(f; \boldsymbol{f}_n) &= \boldsymbol{y}^{\mathrm{H}}(\boldsymbol{P}(f; \boldsymbol{f}_n) - \boldsymbol{P}(\boldsymbol{f}_n))\boldsymbol{y} \\ &= \boldsymbol{y}^{\mathrm{H}}\boldsymbol{P}^{\perp}(\boldsymbol{f}_n)\boldsymbol{d}(\boldsymbol{d}^{\mathrm{H}}\boldsymbol{P}^{\perp}(\boldsymbol{f}_n)\boldsymbol{d})^{-1}\boldsymbol{d}^{\mathrm{H}}\boldsymbol{P}^{\perp}(\boldsymbol{f}_n)\boldsymbol{y}. \end{aligned} \tag{13}$$

4. Notch periodogram analysis

Now we use the results from the previous section and show how to detect multiple and closely spaced sinusoids by using the notch periodogram. For simplicity, first we assume that $l = 1$, i.e., there is one peak in the periodogram at frequency f_n, and $m \leqslant 2$. We will address the cases of $m > 2$ and multiple peaks later.

When there is one peak and $m \leqslant 2$, we have to examine the following hypotheses:

$\mathscr{H}_1$: The data contain one sinusoid under the spectral peak around f_n;

$\mathscr{H}_2$: The data contain two sinusoids under the spectral peak around f_n.

Our objective is to find a relevant statistic when $\mathscr{H}_1$ is true, which will allow for evaluation of the false alarm probability. A statistic that we investigate is based on the maximum value of the notch periodogram in the vicinity of the notch frequency.

To begin, let $\mathscr{H}_1$ be true, that is, the spectral peak at f_n is due to one sinusoid only, $m = 1$. The notch frequency f_n is obtained from

$$f_n = \arg\max_f \boldsymbol{y}^{\mathrm{H}}\boldsymbol{P}(f)\boldsymbol{y} \tag{14}$$

and the notch periodogram of $\boldsymbol{y}$ is expressed by (11). Now, the original spectral peak at f_n disappears from $P_n(f, f_n)$, and $2P_n(f;f_n)/\sigma^2$ has a non-central χ^2 p.d.f. with a non-central parameter

$$\lambda = \frac{2\rho}{N'(\Delta)}\left|\frac{\sin(\pi\Delta_3 N)}{\sin(\pi\Delta_3)} - \frac{1}{N}\frac{\sin(\pi\Delta N)\sin(\pi\Delta_1 N)}{\sin(\pi\Delta)\sin(\pi\Delta_1)}\right|^2, \tag{15}$$

where $\Delta_1 = f_1 - f_n$, $\Delta_3 = f - f_1$, and $\rho = |a_1|^2/\sigma^2$ is the signal-to-noise ratio (SNR). (For the derivation of λ, see Appendix A.) The non-central parameter is always small despite its dependence on the SNR. In particular, we can show that λ increases as $\Delta \to 0$ and write

$$\lambda \leqslant \frac{6\rho}{N^2(N-1)\sin^2(\pi\Delta_1)} \times\left(\frac{\sin(\pi\Delta_1 N)\cos(\pi\Delta_1)}{\sin(\pi\Delta_1)} - N\cos(\pi\Delta_1 N)\right)^2. \tag{16}$$

Note that for high SNR, Δ_1 becomes very small, which offsets the increase in SNR.

Since the noise variance σ^2 is in general unknown, we replace it by its estimate $\hat{\sigma}^2$ defined by

$$\hat{\sigma}^2 = \frac{1}{M_{\mathscr{F}}}\sum_{f\in\mathscr{F}} P_n(f;f_n), \tag{17}$$

where $\mathscr{F} = \{f: f = k/M, |f - f_n| \geqslant (2\mathrm{N})^{-1},\ k = 0, L, 2L, \ldots, (N-1)L\}$, M is the number of equally spaced frequencies (bins) in the range $(0, 1)$ for which we compute the notched periodogram, $M_{\mathscr{F}}$ is the number of bins included in the set $\mathscr{F}$, and $L = [M/N]$ with $[M/N]$ denoting the largest integer that does not exceed M/N. In other words, $\hat{\sigma}^2$ is the mean of $P_n(f;f_n)$ over the range $|f - f_n| \geqslant (2N)^{-1}$. Then $P_n(f;f_n)/\hat{\sigma}^2$ for $f \neq f_n$ has a non-central F p.d.f. with $(2, 2(N-K))$ degrees of freedom and a non-central parameter λ given by (15) ($F_{2,2N-2K}(\lambda)$), where K is the number of bins excluded in evaluating $\hat{\sigma}^2$ and is equal to the number of signal peaks in the periodogram.[2]

Next we derive the p.d.f. of the maximum value of $P_n(f;f_n)/\hat{\sigma}^2$ in the range $|\Delta| < (2N)^{-1}$. Since $P_n(f;f_n)/\hat{\sigma}^2$ is a smooth curve in the neighborhood of the notch frequency, the local maxima of $P_n(f;f_n)/\hat{\sigma}^2$ in $0 < \Delta < (2N)^{-1}$ and $-(2N)^{-1} < \Delta < 0$, denoted by p_{n1} and p_{n2} respectively, will be located with high probability around $f_n \pm (2N)^{-1}$. If p_{n1} and p_{n2} were independent, $p_{\max}^{(1)} = \max(p_{n1}, p_{n2})$ would be distributed according to (Eqs. (8)–(14) on p. 185 of [11])

$$g_{p_{\max}^{(1)}}(p) = 2g(p)G(p), \tag{18}$$

where $g(p)$ is $F_{2,2N-2K}(\lambda)$ and $G(p)$ is the cumulative distribution function (c.d.f.) of $F_{2,2N-2K}(\lambda)$. The superscript $^{(1)}$ of $p_{\max}^{(1)}$ denotes the number of components in the notch set. However, p_{n1} and p_{n2} are weakly correlated, and the maximum value of $P_n(f;f_n)/\hat{\sigma}^2$ in the range $|\Delta| < (2N)^{-1}$, $p_{\max}^{(1)}$, will not be exactly distributed according to (18).

To get a better insight into the above conjectures, we made the following test. We generated one sinusoid, $m = K = 1$, of length $N = 25$, embedded in zero mean white Gaussian noise according to the model definition in (1). The amplitude of the sinusoid was $a_1 = 1$ and the frequency was $f_1 = 0.5 + (2M)^{-1}$, where M was 1024 and was the number of points for which we evaluated the whole periodogram. The SNR, defined by $\mathrm{SNR} = 10\log_{10}(|a_1|^2/\sigma^2)$, was equal to 0 dB. There were 1000 independent trials in the experiment. The empirical c.d.f. of $2P_n(f;f_n)/\sigma^2$ and $P_n(f;f_n)/\hat{\sigma}^2$ with $f = (2N)^{-1} + f_n$ are shown in Fig. 1(a) and (b) plotted together with the hypothesized χ_2^2 central and $F_{2,2N-2}$ c.d.f.'s, respectively. We then applied a Kolmogorov goodness of fit test to verify our distributional assumptions [3]. For a critical value of $\alpha = 0.05$ and 1000 trials, the Kolmogorov statistic is 0.042 [3], which is plotted in Fig. 1(a) and (b)

[2] For a definition of the non-central F p.d.f., its relation to other functions, and ways of computing it, see, for example, [1].

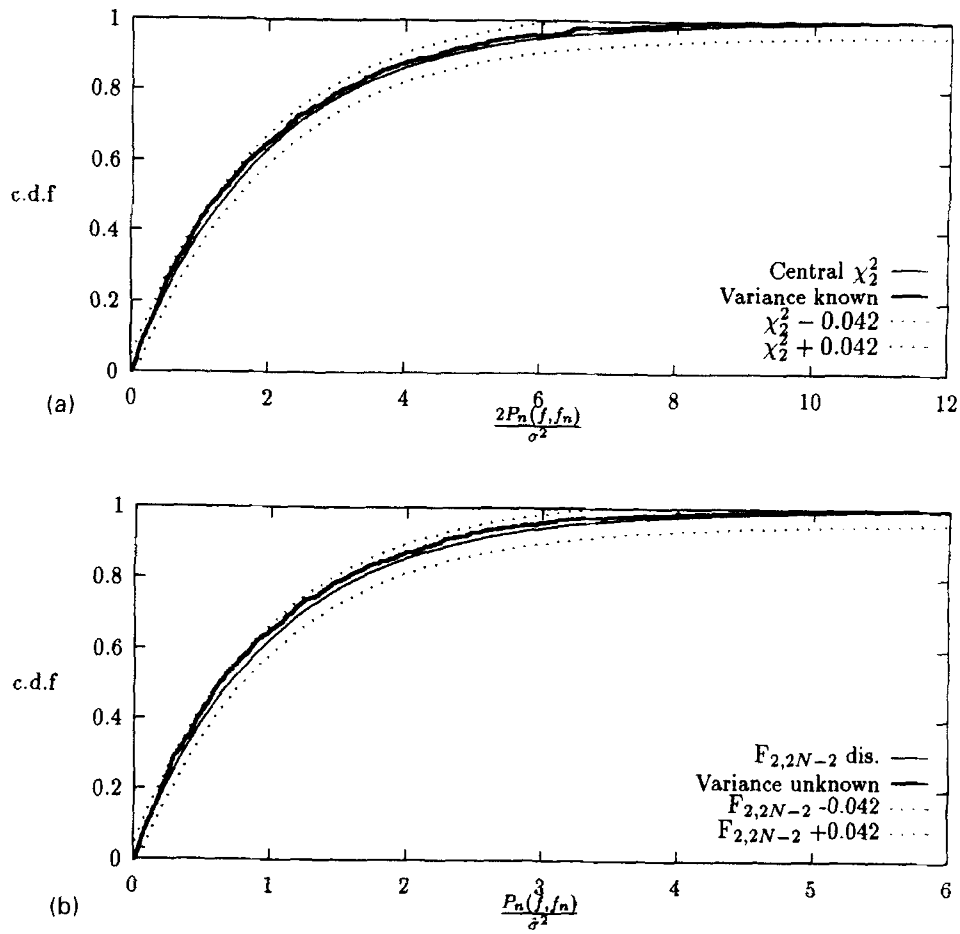

Fig. 1. Comparison of (a) the empirical c.d.f. of $2P_n(f;f_n)/\sigma^2$ with the hypothesized central χ_2^2 c.d.f., and (b) the empirical c.d.f. of $P_n(f;f_n)/\hat{\sigma}^2$ with the $F_{2,2N-2}$ c.d.f.

with dashed lines. It is clear that the maximum difference between the empirical and the hypothesized c.f.d.'s in Fig. 1(a) and (b) is smaller than 0.042.

In Fig. 2(a) and (b), we display the empirical c.d.f. of $p_{\max}^{(1)}$ together with the c.d.f. from (18) and the empirical c.d.f. of $2p_{\max}^{(1)}$ with the central χ_2^2 c.d.f., respectively. As expected, the empirical distributions and the ones obtained from (18) do not pass the Kolmogorov test. However, in the tails, they almost coincide, in particular when $g(p)$ in (18) is the χ_2^2 c.d.f. So, to decide between the hypotheses that there is one ($\mathscr{H}_1$) or more than one sinusoids ($\mathscr{H}_{a_1}$) under the peak, we use the test

$$p_{\max}^{(1)} = \max_{|f-f_n|<(2N)^{-1}} \frac{2P_n(f;f_n)}{\hat{\sigma}^2} \underset{\mathscr{H}_1}{\overset{\mathscr{H}_{a_1}}{\gtrless}} \gamma_1, \tag{19}$$

where γ_1 is a threshold obtained from the χ_2^2 distribution.

Now we consider the case where $\mathscr{H}_2$ is true. In this case, the single spectral peak is between f_1 and f_2. Again, let f_n in (11) be the frequency corresponding to the spectral peak and set $\Delta_1 = f_1 - f_n$ and $\Delta_2 = f_2 - f_n$. Then for high SNR the notch periodogram should have a peak or two peaks at or near

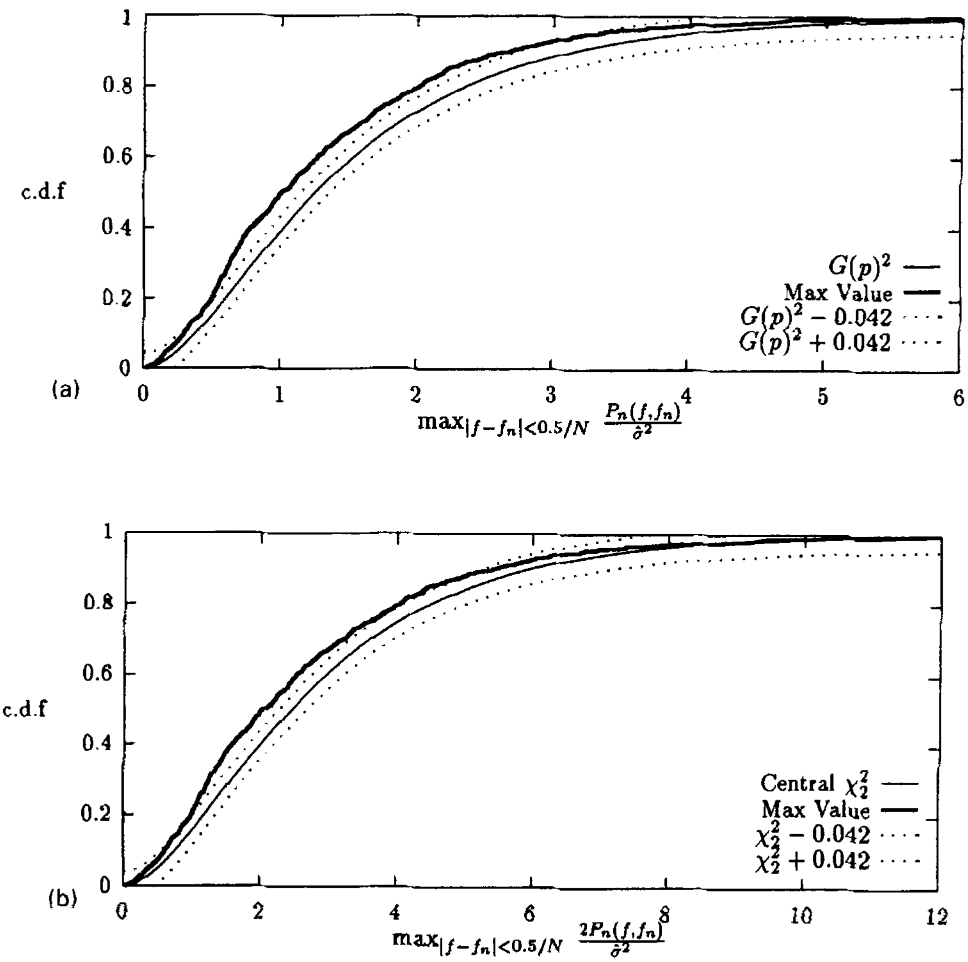

Fig. 2. Comparison of (a) the empirical c.d.f. of $p_{\max}^{(1)}$ with the c.d.f. of (17), $G(p)^2$, and (b) the empirical c.d.f. of $p_{\max}^{(1)}$ with the central χ_2^2 c.d.f.

f_1 or f_2. If we suppose that the peak is at f_1 for example, it is of interest to determine the c.d.f. of $P_n(f;f_n)/\hat{\sigma}^2$, where the notch periodogram at f_1 can be expressed as

$$P_n(f;f_n) = \frac{1}{N'(\Delta_1)}|\boldsymbol{d}^{\mathrm{H}}(f_1)\boldsymbol{P}^{\perp}(f_n)(a_1\boldsymbol{d}(f_1) + a_2\boldsymbol{d}(f_2) + \boldsymbol{\varepsilon})|^2, \quad \Delta_1 \neq 0. \tag{20}$$

For simplicity in the derivation, we assume $a_2 = a_1 \exp(\mathrm{j}\theta)$ and $f_n \simeq (f_1 + f_2)/2$. Then it is not difficult to show that $P_n(f;f_n)/\hat{\sigma}^2$ has approximately non-central $F_{2,2N-2}$ p.d.f. with a non-central parameter λ given by (cf. Appendix B)

$$\lambda = \frac{2\rho}{N'(\Delta_1)}\left|N - \frac{1}{N}\frac{\sin^2(\pi\Delta_1 N)}{\sin^2(\pi\Delta_1)} - \exp(\mathrm{j}\theta_1)\left(\frac{1}{N}\frac{\sin^2(\pi\Delta_1 N)}{\sin^2(\pi\Delta_1)} - \frac{\sin(\pi\Delta_{21}N)}{\sin(\pi\Delta_{21})}\right)\right|^2, \tag{21}$$

where $\Delta_{21} = f_2 - f_1$, and $\theta_1 = \theta + \pi\Delta_{21}(N-1)$. From the criterion (19), it is clear that the algorithm

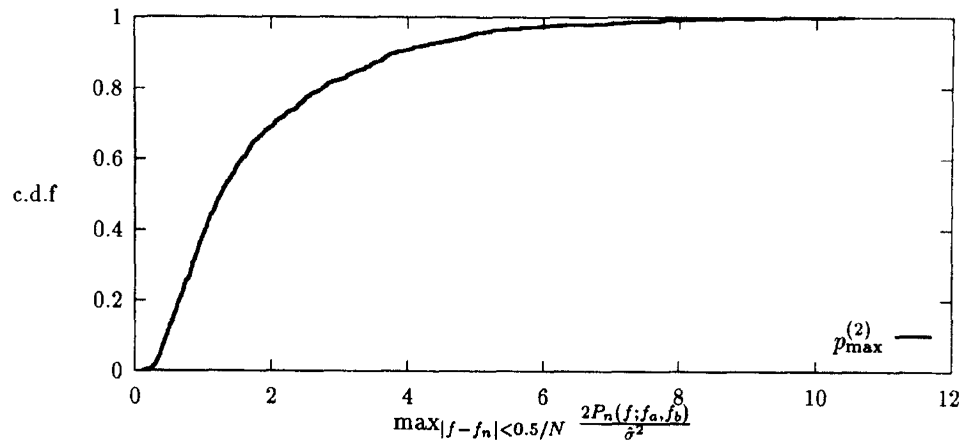

Fig. 3. The empirical c.d.f. of $p^{(2)}_{\max}$.

will select the hypothesis $\mathscr{H}_{a_1}$ with high probability, provided $\mathscr{H}_2$ is true, if the maximum value $p^{(1)}_{\max}$ has a p.d.f. with most of its mass to the right of the threshold γ_1. From the non-central parameter in (21), one can determine the needed SNR (for fixed θ_1) to detect closely spaced sinusoids with a predefined probability. Of course, the higher the predefined probability, the higher the necessary SNR. In addition, from

$$\arg_{\theta_1} \max \lambda = \pi, \qquad \arg_{\theta_1} \min \lambda = 2\pi,$$

and the expression for θ_1 we conclude that the best resolution for fixed f_1 and f_2 is obtained for $\theta = \pi - \pi(f_2 - f_1)(N-1)$, and the worst for $\theta = 2\pi - \pi(f_2 - f_1)(N-1)$. Identical results were obtained in [15] with a more complicated approach where the time index of the data model starts from $n = 1$ instead of $n = 0$ as in our case.

Similarly to (19), we define the next criterion

$$p^{(2)}_{\max} = \max_{|f-f_n|<(2N)^{-1}} \frac{2P_n(f;f_a,f_b)}{\hat{\sigma}^2} \underset{\mathscr{H}_2}{\overset{\mathscr{H}_{a_2}}{\gtrless}} \gamma_2, \tag{22}$$

where $\mathscr{H}_{a_2}$ is the alternative hypothesis to $\mathscr{H}_2$ (the detected number of sinusoids $\hat{m} > 2$), γ_2 denotes the appropriate threshold that satisfies a predefined probability of false alarm, and $P_n(f;f_a,f_b)$ is the notch periodogram with a notch set (f_a, f_b) with f_a and f_b corresponding to the frequencies of the two strongest peaks in $P_n(f;f_n)$ in the range $|f-f_n| < (2N)^{-1}$. We have found that the c.d.f. of $p^{(2)}_{\max}$ is similar to the one of $p^{(1)}_{\max}$. However, its tails are not as significant, which entails that the threshold γ_2 has to be smaller than γ_1. We have conducted extensive investigation of the empirical c.d.f. of $p^{(2)}_{\max}$ for various SNR's and signal parameters. Our results show that for SNR's above 0 dB, this c.d.f. has a shape which for all practical purposes remains free from variations as the SNR or the signal parameters change. This then allows appropriate determination of the new threshold γ_2. In Fig. 3 we show the empirical c.d.f. of $p^{(2)}_{\max}$, and in Table 1 we provide thresholds for given probabilities of false alarm, P_{FA}.

5. Detection algorithm

When we hypothesize more than two sinusoids under one peak, we can still use the proposed procedure. Here we outline its steps under the assumption that $l = 1$ in (2). The case of $l > 1$ is addressed at the end of this section.

If $l = 1$ and we have more than two hypotheses, that is $\mathscr{H}_1, \mathscr{H}_2, \ldots, \mathscr{H}_q$, where $q > 2$, we proceed according to the following steps:

(1) Find the periodogram peak, $f_a^{(0)}$.
(2) Evaluate the notch periodogram with respect to the notch $f_a^{(0)}$ and find the frequency $f_b^{(1)}$

Table 1
The required threshold, γ_2, for a given false alarm probability

P_{FA}	0.01	0.02	0.03	0.04	0.05	0.06	0.07	0.08	0.09	1.00
γ_2	8.0	7.0	6.0	5.2	4.9	4.7	4.5	4.2	4.0	3.8

corresponding to the maximum value, $p_{\max}^{(1)}$, in the range $|f - f_a^{(0)}| < (2N)^{-1}$.

(3) If σ^2 is known, compare $p_{\max}^{(1)} = 2P_n(f_b^{(1)}, f_a^{(0)})/\sigma^2$ with the threshold γ_1, chosen appropriately from the χ_2^2 c.d.f. (We chose the χ_2^2 c.d.f. since it provides good approximation of $g_{p_{\max}^{(1)}}(p)$ in the tails.) If the noise variance is unknown, estimate it according to (17) and compare the maximum value $p_{\max}^{(1)} = 2P_n(f_b^{(1)}; f_a^{(0)})/\hat{\sigma}^2$ with γ_1.

(4) If in step 3 $p_{\max}^{(1)} < \gamma_1$, stop and conclude that there is only one sinusoid, i.e., $\hat{m} = 1$. Otherwise, find the two largest peaks of the notch periodogram $(f_a^{(1)}, f_b^{(1)})$ (if there is only one peak, at say $f_b^{(1)}$, set $f_a^{(1)} = f_a^{(0)}$).

(5) Find the new notch periodogram with respect to the notch vector $(f_a^{(1)}, f_b^{(1)})$.

(6) Compare the maximum value of the new notch periodogram $p_{\max}^{(2)} = \max_f 2P_n(f; f_a^{(1)}, f_b^{(1)})/\sigma^2$, where $|f - f_a^{(0)}| < (2N)^{-1}$, with the threshold γ_2. If σ^2 is unknown, estimate it by

$$\hat{\sigma}^2 = \frac{1}{M_{\mathscr{F}}} \sum_{f \in \mathscr{F}} P_n(f; f_a^{(1)}, f_b^{(1)}), \tag{23}$$

where $\mathscr{F} = \{f\colon\ f = k/M, |f - f_a^{(0)}| \geqslant (2N)^{-1}, k = 0, L, 2L, \ldots, (N-1)L\}$, and $M_{\mathscr{F}}$ is the number of bins in the set $\mathscr{F}$.

(7) If the maximum value in step 6 is less than γ_2, then stop, there are only two sinusoids, i.e., $\hat{m} = 2$. Otherwise, find the three peaks of the new notch periodogram, $(f_a^{(2)}, f_b^{(2)}, f_c^{(2)})$, similarly as in step 4. Continue along the same lines until the test fails to support further increase of hypothesized sinusoids. The appropriate thresholds γ_3, γ_4 and so on, are determined empirically as γ_2.

If $l > 1$, the detection algorithm for the kth peak is similar to the one that was outlined. There are two differences. First, when the kth peak is analyzed, each notch periodogram has also notches at the other peaks of the original periodogram. Second, the frequency set $\mathscr{F}$ used for estimation of σ^2 is changed to exclude the regions around the peaks of the periodogram.

6. Simulation result

In this section, we present some simulation results to demonstrate the NPD performance. We consider four examples, one with a single, two with two sinusoids, and three sinusoids in the last example. For the first example, the complex data were generated according to

$$y[n] = \exp(\mathrm{j}(2\pi 0.51n + \pi/4)) + \varepsilon[n] \tag{24}$$

and for the second by

$$y[n] = \exp(\mathrm{j}2\pi 0.5n) + \exp(\mathrm{j}(2\pi 0.51n + \pi/4)) + \varepsilon[n]. \tag{25}$$

The data in the third example were obtained by

$$y[n] = \exp(\mathrm{j}2\pi 0.5n) + 1/\sqrt{10}\exp(\mathrm{j}(2\pi 0.51n + \pi/4)) + \varepsilon[n] \tag{26}$$

and in the fourth by

$$y[n] = \exp(\mathrm{j}2\pi 0.5n) + \exp(\mathrm{j}(2\pi 0.51n + \pi/4)) + \exp(\mathrm{j}(2\pi 0.53n + \pi/16)) + \varepsilon[n]. \tag{27}$$

In all examples $n = 0, 1, \ldots, 24$, and the SNR was varied between 0 and 20 dB. For each SNR there were 200 trials and we chose $\gamma_1 = 7$ and $\gamma_2 = 6$ which correspond to $P_{FA} = 0.03$. Note that in the second and third experiments, the sinusoids were separated by half of the resolution limit. Also, in the fourth experiment there are three sinusoids in one

Table 2
Detection performance of the NPD method when $m = 1$. The numbers denote the estimated probabilities of detecting $\hat{m} = 1, 2$ and 3 sinusoids for SNR's in the range from 0 to 20 dB

	$\hat{m}$		
SNR (dB)	1	2	3
0	0.985	0.015	0.000
1	0.995	0.005	0.000
2	0.990	0.010	0.000
3	0.990	0.010	0.000
4	0.980	0.020	0.000
5	0.980	0.020	0.000
6	0.985	0.015	0.000
7	0.990	0.010	0.000
8	0.990	0.010	0.000
9	0.970	0.030	0.000
10	0.985	0.015	0.000
11	0.985	0.015	0.000
12	0.995	0.005	0.000
13	0.985	0.015	0.000
14	0.995	0.005	0.000
15	1.000	0.000	0.000
16	0.985	0.015	0.000
17	0.990	0.010	0.000
18	1.000	0.000	0.000
19	0.985	0.015	0.000
20	0.980	0.020	0.000

Table 3
Detection performance of the NPD method when $m = 2$ and the amplitudes of the two sinusoids are the same. The numbers denote the estimated probabilities of detecting $\hat{m} = 1, 2$ and 3 sinusoids for SNR's in the range from 0 to 20 dB

	$\hat{m}$		
SNR (dB)	1	2	3
0	0.650	0.350	0.000
1	0.450	0.545	0.005
2	0.315	0.685	0.000
3	0.195	0.800	0.005
4	0.165	0.835	0.000
5	0.045	0.955	0.000
6	0.020	0.980	0.000
7	0.000	0.995	0.005
8	0.000	0.995	0.005
9	0.000	0.995	0.005
10	0.000	1.000	0.000
11	0.000	1.000	0.000
12	0.000	1.000	0.000
13	0.000	1.000	0.000
14	0.000	1.000	0.000
15	0.000	0.995	0.005
16	0.000	1.000	0.000
17	0.000	1.000	0.000
18	0.000	1.000	0.000
19	0.000	1.000	0.000
20	0.000	1.000	0.000

periodogram peak, that is $m_1 = 3$. The detection results are presented in Tables 2–5, respectively.

From Table 2 we see that the algorithm has excellent performance throughout the whole SNR range. The estimated probabilities of false alarm are between 0 and 0.03. The results of the experiment with two sinusoids that have equal amplitudes are shown in Table 3. The algorithm has very good performance for SNR's above 5 dB. For SNR below 5 dB, and as it decreases, the algorithm tends to select with increased probability one sinusoid only. The results of the third experiment are given in Table 4. Note that the amplitudes of the two sinusoids differ by 10 dB, and that the SNR is defined according to the stronger sinusoid. The performance is excellent for SNR's greater than 13 dB and starts to deteriorate as it gets smaller. This is not surprising because it is well known from estimation theory that the frequency estimates of the sinusoids begin to deteriorate considerably at about 3 dB [9], which is in our example the SNR of the weaker sinusoid. Finally, the results of the fourth experiment are given in Table 5. In the scenario of three closely spaced sinusoids, the performance is satisfactory for SNR's greater than 17 dB.

7. Conclusions

We presented the derivation of a simple algorithm that can be used to detect closely space sinusoids. This algorithm is based on the notch periodogram and can be implemented by the FFT. The algorithm processes each peak of the periodogram separately. In examining each peak, it starts with the hypothesis of one sinusoid under the peak, and continues with two, three, etc. sinusoids until

Table 4
Detection performance of the NPD method when $m = 2$ and the amplitudes of the two sinusoids are related by $a_2 = a_1 e^{j\pi/4}/\sqrt{10}$. The numbers denote the estimated probabilities of detecting $\hat{m} = 1, 2$ and 3 sinusoids for SNR's in the range from 0 to 20 dB. The SNR is measured with respect to the first sinusoid

	$\hat{m}$		
SNR (dB)	1	2	3
0	0.945	0.055	0.000
1	0.905	0.095	0.000
2	0.865	0.135	0.000
3	0.785	0.215	0.000
4	0.825	0.175	0.000
5	0.690	0.310	0.000
6	0.680	0.320	0.000
7	0.660	0.340	0.000
8	0.475	0.515	0.010
9	0.380	0.610	0.010
10	0.325	0.675	0.000
11	0.170	0.825	0.005
12	0.105	0.895	0.000
13	0.025	0.975	0.000
14	0.005	0.995	0.000
15	0.000	1.000	0.000
16	0.000	0.990	0.010
17	0.000	1.000	0.000
18	0.000	1.000	0.000
19	0.000	0.995	0.005
20	0.000	1.000	0.000

Table 5
Detection performance of the NPD method when $m = 3$ and the amplitudes of the three sinusoids are the same. The numbers denote the estimated probabilities of detecting $\hat{m} = 1, 2, 3$ and 4 sinusoids for SNR's in the range from 0 to 20 dB

	$\hat{m}$			
SNR (dB)	1	2	3	4
0	0.000	0.970	0.030	0.000
1	0.000	0.990	0.010	0.000
2	0.000	0.980	0.020	0.000
3	0.000	0.985	0.015	0.000
4	0.000	0.990	0.010	0.000
5	0.000	0.980	0.020	0.000
6	0.000	0.975	0.025	0.000
7	0.000	0.945	0.055	0.000
8	0.000	0.900	0.100	0.000
9	0.000	0.800	0.200	0.000
10	0.000	0.720	0.280	0.000
11	0.000	0.630	0.370	0.000
12	0.000	0.415	0.585	0.000
13	0.000	0.270	0.730	0.000
14	0.000	0.145	0.845	0.010
15	0.000	0.080	0.915	0.005
16	0.000	0.030	0.960	0.010
17	0.000	0.005	0.985	0.010
18	0.000	0.000	0.995	0.005
19	0.000	0.000	0.995	0.005
20	0.000	0.000	1.000	0.000

the newest hypothesis is rejected. The experimental results showed agreement with our analysis as well as excellent performance.

Appendix A

Proposition. *If* $y = a_1 d(f_1) + \varepsilon$, *where* $d^T = [1 \ \exp(j2\pi f_1) \ \exp(j4\pi f_1) \ldots \exp(j(N-1)2\pi f_1)]$, a_1 *is a complex constant, and* $\varepsilon \sim CN(\mathbf{0}, \sigma^2 \mathbf{I})$ *with the real and imaginary components identically distributed, then for* $f \neq f_n$, *the random variable* $2P_n(f; f_n)/\sigma^2$, *where* $P_n(f; f_n)$ *is the notch periodogram of* y *defined by* (11) *has a non-central* χ^2 *p.d.f. with two degrees of freedom and a non-central parameter given by* (15).

Proof. Recall that the notch periodogram was defined as

$$P_n(f; f_n) = \frac{1}{N'(\Delta)} |\boldsymbol{d}^{\mathrm{H}}(f) \boldsymbol{P}^{\perp}(f_n) \boldsymbol{y}|^2. \tag{A.1}$$

Now we substitute for $\boldsymbol{y}$, $a_1 \boldsymbol{d}(f_1) + \boldsymbol{\varepsilon}$, and obtain

$$\begin{aligned} P_n(f; f_n) &= \frac{1}{N'(\Delta)} |\boldsymbol{d}^{\mathrm{H}}(f) \boldsymbol{P}^{\perp}(f_n)(a_1 \boldsymbol{d}(f_1) + \boldsymbol{\varepsilon})|^2 \\ &= \frac{1}{N'(\Delta)} |a_1 \boldsymbol{d}^{\mathrm{H}}(f) \boldsymbol{P}^{\perp}(f_n) \boldsymbol{d}(f_1) \\ &\quad + \boldsymbol{d}^{\mathrm{H}}(f) \boldsymbol{P}^{\perp}(f_n) \boldsymbol{\varepsilon}|^2 \\ &= \frac{1}{N'(\Delta)} \Bigg\{ \Bigg(\mathrm{Re} \Bigg[a_1 \boldsymbol{d}^{\mathrm{H}}(f) \boldsymbol{P}^{\perp}(f_n) \boldsymbol{d}(f_1) \\ &\quad + \boldsymbol{d}^{\mathrm{H}}(f) \boldsymbol{P}^{\perp}(f_n) \boldsymbol{\varepsilon} \Bigg] \Bigg)^2 \end{aligned}$$

$$+\left(\mathrm{Im}\left[a_1\boldsymbol{d}^{\mathrm{H}}(f)\boldsymbol{P}^{\perp}(f_n)\boldsymbol{d}(f_1)+\boldsymbol{d}^{\mathrm{H}}(f)\boldsymbol{P}^{\perp}(f_n)\boldsymbol{\varepsilon}\right]\right)^2\Bigg\}, \tag{A.2}$$

where Re[ ] and Im[ ] denote the real and imaginary components of a complex number. Since $\mathrm{Re}[\boldsymbol{\varepsilon}] \sim N(0,(\sigma^2/2)\boldsymbol{I})$, $\mathrm{Im}[\varepsilon] \sim N(0,(\sigma^2/2)\boldsymbol{I})$, and $\mathrm{Re}[\boldsymbol{\varepsilon}]$ is independent of $\mathrm{Im}[\boldsymbol{\varepsilon}]$, it is easy to show that

$$\mathrm{Re}\left[a_1\boldsymbol{d}^{\mathrm{H}}(f)\boldsymbol{P}^{\perp}(f_n)\boldsymbol{d}(f_1)+\boldsymbol{d}^{\mathrm{H}}(f)\boldsymbol{P}^{\perp}(f_n)\boldsymbol{\varepsilon}\right] \sim N\left(\mathrm{Re}\left[a_1\boldsymbol{d}^{\mathrm{H}}(f)\boldsymbol{P}^{\perp}(f_n)\boldsymbol{d}(f_1)\right], \frac{N'(\Delta)\sigma^2}{2}\right),$$
$$\mathrm{Im}\left[a_1\boldsymbol{d}^{\mathrm{H}}(f)\boldsymbol{P}^{\perp}(f_n)\boldsymbol{d}(f_1)+\boldsymbol{d}^{\mathrm{H}}(f)\boldsymbol{P}^{\perp}(f_n)\boldsymbol{\varepsilon}\right] \sim N\left(\mathrm{Im}\left[a_1\boldsymbol{d}^{\mathrm{H}}(f)\boldsymbol{P}^{\perp}(f_n)\boldsymbol{d}(f_1)\right], \frac{N'(\Delta)\sigma^2}{2}\right). \tag{A.3}$$

Therefore, $2P_n(f;f_n)/\sigma^2$ has non-central χ^2 p.d.f. with two degrees of freedom with the non-central parameter λ given by

$$\lambda = \frac{2}{N'(\Delta)\sigma^2}\left(\mathrm{Re}^2\left[a_1\boldsymbol{d}^{\mathrm{H}}(f)\boldsymbol{P}^{\perp}(f_n)\boldsymbol{d}(f_1)\right] + \mathrm{Im}^2\left[a_1\boldsymbol{d}^{\mathrm{H}}(f)\boldsymbol{P}^{\perp}(f_n)\boldsymbol{d}(f_1)\right]\right)$$
$$= \frac{2}{N'(\Delta)\sigma^2}\,|a_1\boldsymbol{d}^{\mathrm{H}}(f)\boldsymbol{P}^{\perp}(f_n)\boldsymbol{d}(f_1)|^2$$
$$= \frac{2|a_1|^2}{N'(\Delta)\sigma^2}\left|\sum_{n=0}^{N-1}\exp(\mathrm{j}2\pi(f_1-f)n) - \frac{1}{N}\sum_{n=0}^{N-1}\exp(\mathrm{j}2\pi(f_n-f)n) \times \sum_{n=0}^{N-1}\exp(\mathrm{j}2\pi(f_1-f_n)n)\right|^2$$
$$= \frac{2\rho}{N'(\Delta)}\left|\exp(-\mathrm{j}\pi\Delta_3(N-1))\frac{\sin\pi\Delta_3 N}{\sin\pi\Delta_3} - \exp(\mathrm{j}\pi(\Delta_1-\Delta)(N-1)) \times\frac{1}{N}\frac{\sin\pi\Delta N\sin\pi\Delta_1 N}{\sin\pi\Delta\sin\pi\Delta_1}\right|^2$$
$$= \frac{2\rho}{N'(\Delta)}\left|\frac{\sin(\pi\Delta_3 N)}{\sin(\pi\Delta_3)} - \frac{1}{N}\frac{\sin(\pi\Delta N)\sin(\pi\Delta_1 N)}{\sin(\pi\Delta)\sin(\pi\Delta_1)}\right|^2, \tag{A.4}$$

where $\Delta = f - f_n$, $\Delta_1 = f_1 - f_n$, and $\Delta_3 = f - f_1$. □

Appendix B

Here we show that $P_n(f;f_n)/\hat{\sigma}^2$ in (20), under the assumption $f_n = (f_1 + f_2)/2$ and $a_2 = a_1\exp(\mathrm{j}\theta)$ has a non-central $F_{2,2N-2}$ p.d.f. with non-central parameter λ given by (21).

Clearly, $2P_n(f;f_n)/\sigma^2$ has a non-central χ_2^2 p.d.f. whose non-central parameter is derived in the sequel. On the other hand, $2(N-1)\hat{\sigma}^2/\sigma^2$ has approximately a central $\chi^2_{2(N-1)}$ p.d.f. Since $2P_n(f_1;f_n)/\sigma^2$ and $2(N-1)\hat{\sigma}^2/\sigma^2$ are independent, it follows straightforwardly that $P_n(f_1;f_n)/\hat{\sigma}^2$ has an $F_{2,2(N-1)}$ p.d.f.

Next, we derive the non-central parameter λ. We can write

$$\lambda = \frac{2}{N'(\Delta_1)\sigma^2}|\boldsymbol{d}^{\mathrm{H}}(f_1)\boldsymbol{P}^{\perp}(f_n)(a_1\boldsymbol{d}(f_1)+a_2\boldsymbol{d}(f_2))|^2$$
$$= \frac{2}{N'(\Delta_1)\sigma^2}\,|\boldsymbol{d}^{\mathrm{H}}(f_1)(a_1\boldsymbol{d}(f_1)+a_1\exp(\mathrm{j}\theta)\boldsymbol{d}(f_2)) - \frac{1}{N}\boldsymbol{d}^{\mathrm{H}}(f_1)\boldsymbol{d}(f_n)\boldsymbol{d}^{\mathrm{H}}(f_n)(a_1\boldsymbol{d}(f_1) + a_1\exp(\mathrm{j}\theta)\boldsymbol{d}_2\}|^2$$
$$= \frac{2\rho}{N'(\Delta_1)}\left|N + \sum_{n=0}^{N-1}\exp(\mathrm{j}(\theta+2\pi\Delta_{21}n)) - \frac{1}{N}\sum_{n=0}^{N-1}\exp(-\mathrm{j}2\pi\Delta_1 n_1)\left(\sum_{n=0}^{N-1}\exp(\mathrm{j}2\pi\Delta_1 n\right) + \sum_{n=0}^{N-1}\exp(\mathrm{j}(\theta+2\pi\Delta_2 n))\right|^2$$

$$= \frac{2\rho}{N'(\Delta_1)} \left| N\left(1 + \exp(j\theta_1)\frac{\sin(\pi\Delta_{21}N)}{N\sin(\pi\Delta_{21})}\right) - \frac{1}{N}\frac{\sin^2(\pi\Delta_1 N)}{\sin^2(\pi\Delta_1)}(1+\exp j\theta_1)\right|^2$$

$$= \frac{2\rho}{N'(\Delta_1)} \left| N - \frac{1}{N}\frac{\sin^2(\pi\Delta_1 N)}{\sin^2(\pi\Delta_1)} - \exp(j\theta_1)\left(\frac{1}{N}\frac{\sin^2(\pi\Delta_1 N)}{\sin^2(\pi\Delta_1)} - \frac{\sin(\pi\Delta_{21}N)}{\sin(\pi\Delta_{21})}\right)\right|^2, \tag{B.1}$$

where $\Delta_{21} = f_2 - f_1$, θ is the phase difference between s_1 and s_2 and $\theta_1 = \theta + 2\pi\Delta_1(N-1)$.

References

[1] M. Abramowitz and I.A. Stegun, *Handbook of Mathematical Functions*, Dover, New York, 1970, pp. 946 and 961.

[2] H. Akaike, "A new look at the statistical model identification", *IEEE Trans. Automatic Control*, Vol. 19, No. 6, December 1974, pp. 716–723.

[3] P.J. Bickel and K.A. Doksum, *Mathematical Statistics*, Holden-Day, San Francisco, CA, 1977, Chapter 9, pp. 378–381.

[4] P.M. Djurić, "Simultaneous detection and frequency estimation of sinusoidal signals", *Proc. Internat. Conf. Acoust. Speech Signal Process.*, Vol. IV, 1993, pp. 53–56.

[5] M.L. Honig and D.G. Messerschmitt, *Adaptive Filters Structure, Algorithms, and Applications*, Kluwer, Dordrecht, 1984, Chapter 6, pp. 145–160.

[6] J.-K. Hwang and Y.-C. Chen, "A combined detection–estimation algorithm for the harmonic-retrieval problem", *Signal Processing*, Vol. 30, No. 2, January 1993, pp. 177–197.

[7] J.K. Hwang and Y.C. Chen, "Superresolution frequency estimation by alternating notch periodogram', *IEEE Trans. Signal Process.*, Vol. 41, No. 2, February 1993, pp. 727–741.

[8] D.E. Johnston and P.M. Djurić, "Bayesian detection and MMSE frequency estimation of sinusoidal signal via adaptive importance sampling", *Proc. Internat. Symposium Circuits and Systems*, Vol. 2, London, England, 1994, pp. 417–420.

[9] S. Kay, *Modern Spectrum Estimation: Theory and Application*, Prentice-Hall, Englewood Cliffs, NJ, Chapter 13, pp. 436–438.

[10] J.S. Lim and A.V. Oppenheim, eds., *Advanced Topics in Signal Processing*, Prentice-Hall, Englewood Cliffs, NJ, Chapter 2, pp. 58–87.

[11] A. Papoulis, *Probability, Random Variables, and Stochastic Process*, McGraw-Hill, New York, 1991, 3rd Edition, Chapter 8, pp. 185–186.

[12] B.G. Quinn, "Testing for the presence of sinusoidal components", *Applied Probability Trust*, 1986, pp. 201–210.

[13] J. Rissanen, "Modelling by shortest data description", *Automatica*, Vol. 14, 1978, pp. 465–471.

[14] X. Wang, "An AIC type estimator for the number of cosinusoids", *J. Time Series Analysis*, Vol. 14, No. 4, 1993, pp. 433–440.

[15] D.M. Wilkes and J.A. Cadzow, "The effects of phase on high-resolution frequency estimators", *IEEE Trans. Signal Process.*, Vol. 41, No. 3, March 1993, pp. 1319–1330.

[16] C.J. Ying, L.C. Potter and R.L. Moses, "On model order determination for complex exponential signals: Performance of an FFT-initialized ML algorithm", *Proc. 7th SP Workshop on Statistical Signal and Array Processing*, Quebec, Canada, 26–29 June 1994, pp. 43–46.